International Journal of Current Microbiology and Applied Sciences
ISSN: 2319-7706 **Volume 4 Number 3 (2015) pp. 5-19**
http://www.ijcmas.com

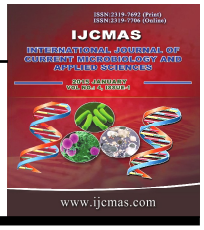

Original Research Article

In vitro and *in vivo* antibacterial potential of chitosan - g - acrylonitrile silver nanocomposite against a pathogenic bacterium

A. Hebeish[1], M.A. Ramadan[1], I. krupa[4], A.S. Montaser[1]*, Abeer A. A. Salama[2] and M.S. Abdel-Aziz[3]

[1]National Research Centre, Textile Research Division, Dokki, Cairo, Egypt
[2]National Research Centre, Pharmacology Department, Dokki, Cairo, Egypt
[3]National Research Centre, Microbial Chemistry Department, Dokki, Cairo, Egypt
[4]Polymer Institute, Slovak academy of science, Bratislava, Slovakia
**Corresponding author*

Keywords

Alginate beads, Cs-g-PAN/Ag nanocomposite, Antimicrobial activity.

A B S T R A C T

Due to their antibacterial activity and biocompatibility, chitosan and chitosan derivatives have ability of participating in biological applications. The prepared Cs–g-PAN/Ag nanocomposites are reported as antibacterial agents that exhibit efficient antibacterial activity *in vitro*. The prepared chitosan-g- PAN/Ag nanocomposite was provided by FTIR and gravimetric methods. UV spectra and TEM images show silver nanoparticles with average 15–20 nm dispersed homogeneously in (CS-g-PAN/Ag) nanocomposite. The antimicrobial activity examined against gram negative bacterium (*E. coli*) and gram positive bacterium (*Staphylococcus aureus*) in addition to yeast (*Candida albicans*) and fungi (*Aspergillusniger*) is evaluated *in vitro*. The MIC for *E. coli* for *in vivo* application was also examined. In vivo antibacterial activity against *E. coli* has been evaluated by using an intestine-infected rat model. Experimental results indicated that the number of bacteria surviving in the small intestine is lower than in the untreated group. These nanocomposite open up a new avenue for design and synthesis of next-generation antibacterial agents as alternatives to antibiotics.

Introduction

Despite the fact that pathogenic infections are widely treated by antibiotics in the clinic nowadays, the increasing risk of multidrug-resistance associated with abuse of antibiotics became a major concern in global public health. The increased death toll caused by pathogenic bacterial infection calls for effective antibiotic alternatives.

Nanosized inorganic particles, of either simple or composite nature, display unique physical and chemical properties and represent an increasingly important material in the development of novel nanodevices

which can be used in numerous physical, biological, biomedical, and pharmaceutical applications (Chan *et al.,* 2002; Alivisatos, 1996; Akinfieva *et al.,* 2013; Wu *et al.,* 2003). A number of recent achievements offer the possibility of generating new types of nano structured materials with designed surface and structural properties.

The antibacterial effects of silver nanoparticles or Ag nanocomposite have been noticed since antiquity (Brigger *et al.,* 2002), and Ag is currently used to control bacterial growth in a variety of applications, including dental work, catheters, and burn wounds (Akinfieva *et al.,* 2013; Wu *et al.,* 2003). In fact, it is well known that Ag ions and Ag-based compounds are highly toxic to microorganisms, showing strong biocidal effects on as many as 12 species of bacteria including *E. coli* (Brigger *et al.,* 2002).

Nanosized inorganic particles, of either simple or composite nature, display unique physical and chemical properties and represent an increasingly important material in the development of novel nanodevices which can be used in numerous physical, biological, biomedical, and pharmaceutical applications (Chan *et al.,* 2002; Alivisatos, 1996; Akinfieva *et al.,* 2013; Wu *et al.,* 2003; Brigger *et al.,* 2002; Forestier *et al.,* 1992; Sondi *et al.,* 2000; Siiman et al). A number of recent achievements offer the possibility of generating new types of nanostructured materials with designed surface and structural properties (Mattoussi *et al.,* 2011; Joguet *et al.,* 2002; Sondi *et al.,* 2000; Richards *et al.,* 2000; Klabunde *et al.,* 1996).

Our previous study has shown that stable and highly concentrated aqueous dispersions of Cs-g-PAN/Ag nanocomposite of narrow size distribution can be simply prepared by reducing silver ions during grafting process of acrylonitrile onto chitosan chain (Hebeish *et al.,* 2014).

Here we investigate the biocidal action of this nanocomposite against *E. coli*. The ultimate goal was to study the MIC dose for *E. coli* inhibition and this work extends to overview its ability to apply onto animals.

Materials and Methods

Materials

Chitosan (deacetylation 90%, M.Wt; 35000) was supplied by Aldrich Co, Ltd., Egypt, acrylonitrile and potassium persulfate of analytical grade with purity of 98% were used as the monomer and initiator for grafting onto chitosan, all other chemicals were of analytical grade and used without further purification. *E. coli* bacterium (ATCC8739) and all other microbes were obtained from the Microbial Chemistry Department, National Research Center, Egypt. Chlorampheincol was obtained in the form of powder from Cid Company, Egypt. All the other solvents used in the research were laboratory grade.

Animals

Wiser male rats, weighing ranged from 125-150g were obtained from the animal house colony of the National Research Centre, Dokki, Giza, Egypt. The animals were housed in standard metal cages in an air conditioned room at 22 ± 3˚C, 55 ± 5% humidity and provided with standard laboratory diet and water and libitum. Animal procedures were performed in accordance with the Ethics Committee of the National Research Centre and followed the recommendations of the National Institutes of Health Guide for Care and Use of Laboratory Animals.

Materials and Methods

Synthesis of chitosan (Cs) – polyacrylonitrile (PAN) – silver (Ag) nanocomposite (Cs-g-PAN/Ag nanocomposite)

A 250 ml three necked round bottomed flask, magnetic stirrer, thermometer, and reflux condenser in a temperature-controlled oil bath, was used for carrying out the graft copolymerization reaction of acrylonitrile with chitosan. Firstly, a desired quantity of chitosan was dissolved in 1% acetic acid aqueous solution. After the chitosan was fully dissolved, temperature of the system was strictly controlled at the required temperature. Then potassium persulfate powder (0.23 mg) was added into the solution. After 20 min. acrylonitrile was added drop wise (9.3 ml) to the reaction vessel.

The reaction was conducted for 2 hr with stirring continued for another 15 min at room temperature after one hour passed; one gram of silver nitrate salt added to the graft polymerization reaction medium after addition of acrylonitrile. Then the reaction product was precipitated out with double volume of isopropanol, filtered, washed with distilled water, to remove the unmodified soluble low molecular weight chitosan [14]. The obtained powder dried and subjected to Soxhlet refluxing for 8–12 h using N, N-dimethyl formamide (DMF) to solubilize and remove the homopolymer and finally lyophilized. All the samples were absolutely dried before being subjected to characterization.

Characterization

The product from each step was characterized and evaluated according to the standard procedures as follows:

FTIR Spectroscopy

IR spectra were recorded in KBr discs on a Perkin Elmer Spectrum 2000 FTIR spectrometer under dry air at room temperature. Approximately 6 mg of resulted powder was blended with 200 mg of potassium bromide (IR grade) and about 40 mg of the mixture was used to prepare a pellet.

Ultra Violet–Visible (UV–vis) Spectra

UV-vis spectral analysis was done by means of a 50 ANALYTIKA, JENA Spectrophotometer from 200 to 500 nm.

Transmission Electron Microscope (TEM)

TEM was used to assess the potential impact of the modification on the elemental and structural properties of the synthesized Cs-g-PAN/Ag nanocomposite. The TEM analysis was done usingJEOL-JEM-1200 (Japan)

Antimicrobial activity (cup method)

The cup-plate agar diffusion method described by Srinivasan et al (2001) was adopted to assess the antibacterial activity of the prepared Cs-g-PAN/Ag nanocomposite suspended in sterilized distilled water at a concentration of 1mg/ml. One ml of standardized bacterial stock suspensions (10^8–10^9) colony forming units (CFU) per ml was thoroughly mixed with 250 ml of sterile nutrient agar. Twenty ml of the inoculated nutrient agar was distributed into sterile petri-dishes. The agar was left to set and in each plate 3–4 cups, 10 mm in diameter was cut using a sterile cork borer No.4 and the agar disks were removed. Cups were filled with 0.1 ml of samples and were allowed to diffuse at room temperature for 2 h. Both bacterial and yeast test microbes

were grown on nutrient agar (DSMZ1) medium (g/l): beef extract (3), peptone (10), and agar (20). On the other hand, the fungal strain was grown on Czapek–Dox (DSMZ 130) medium (g/l): sucrose (30), $NaNO_3$ (3), $MgSO_4.7H_2O$ (0.5), KCl (0.5), $FeSO_4 \cdot 7H_2O$ (0.001), K_2HPO_4 (1) and agar (20). The plates were then incubated in the upright position at 37°C for 24 h for bacteria and yeast) and at30°C for 48h (for fungi). After incubation the diameter of the results and growth inhibition zones were measured averaged and the mean values were recorded.

MIC measurement by CFU process using *E. coli*

Cs-g-PAN/Ag nanocomposite with different concentrations starting from 0.01 to 0.3gm in 100ml-Erelenmeyer flasks each are containing 20ml nutrient broth. Then 10 µl *E. coli* cell suspensions in distilled water with a CFU value of about 6.5 × 10^6colonies/ml were added. The flasks were incubated at 37°C for 24h on rotary shaker (100rpm). After incubation a serial dilution has been done for each sample (starting with 10^{-1} to 10^{-6}). From each dilution, 100microliters were surface inoculate nutrient agar plates and the plates were incubated at 37°C for 24h. SBs without Cs-g-PAN/Ag nanocomposite were used as a control and its microbiological effect was tested by the same procedure for Cs-g-PAN/Ag nanocomposite.

Acute toxicity study

Cs-g-PAN/Ag nanocomposite was dissolved in distilled water then given orally in graded doses to rat up to 2g/kg (Ramirez *et al.,* 2000). The control group received the same volumes of distilled water. The mortality percentage for extracts was recorded 24 hours later. Observation of rats for 14 days, for any changes in the skin and fur, respiratory, circulatory, autonomic, central nervous systems, somatomotor activity and behavior pattern has been recorded. Particular observation for tremors, convulsions, salivation, diarrhea, lethargy, sleep, and coma were done.

Rat Infection Model

To evaluate the in vivo antibacterial effect of Cs-g-PAN/Ag nanocomposite, the *E. coli* infection model was built (Li and Wang, 2013). Rats were divided into five groups (each of six). The first group received phosphate buffer saline and serves as normal control, the second group treated with single dose of 0.6 ml of *E. coli* with a CFU value of 4.5×10^7/ml, the third group treated with chloramphenicol (22.5 mg/kg) according to paget's formula (Paget and Barnes, 1964) and the fourth and the fifth groups treated with two concentrations of Cs-g-PAN/Ag nanocomposite (50 and 100 mg/kg). Drugs were introduced into animals by gavage, 3 consecutive days after *E. coli* administration. Over the course of infection, the activity and body weight of animals were recorded. After three days, all rat were sacrificed and the small intestines were separated and homogenized in sterile PBS (5mL) containing 1% Triton X-100. Aliquots of diluted homogenized intestinal tissues were plated on agar, on which the grown colonies were counted for analysis.

Result and Discussion

FTIR analysis

Figure 1 shows the FTIR spectra Cs-g-PAN copolymer and Cs-g-PAN/Ag nanocomposite in comparison with original chitosan. Most of the presented peaks are related to carbohydrate structure. The broad and strong absorption peak at around 3429

cm^{-1} (OH and NH stretching), peak at 2874 cm^{-1} (CH stretching), the three peaks at range of 1000- 1157 cm^{-1} (CO stretching) were common in spectra due to the chitosan backbone. The strong peaks at around 2242 cm^{-1} appeared in spectra (b) and (c) were assigned to the stretching absorption of CN, which provide the successful graft copolymerization of chitosan and AN. And the obvious difference of beak intensity between (b) and (c) at around 2242 cm^{-1} indicated that there existed the homopolymerization of AN (homo PAN) during the graft copolymerization. In comparison to grafted loaded silver nanoparticles there is no difference except more sharpness in some peaks. This implies that, no chemical reaction occurs between grafted polymer and silver nanoparticles.

Characterization of (Cs-g-PAN/Ag) nanocomposite

The UV absorption spectra of silver nanoparticles in the Cs-g-PAV/Ag nanocomposite are shown in Figure 2a. The absorption peak that sharply appears at 407 nm is characteristic to the surface Plasmon resonance absorption of Ag nanoparticles. It's confirms that silver nanoparticles are present in matrices of the currently synthesized composite. It is known that surface Plasmon resonance absorption of Ag nanoparticles is very sensitive to particle aggregation, sharply and small size with very little aggregation of silver nanoparticles could be detected in the polymer matrix. TEM micrographs shown in Figure 2b are pertaining to the prepared nanocomposite. Obviously Ag nanoparticles are being embedded in Cs-g-PAN/Ag nanocomposite matrix, all particles exhibits semi spherical morphology, the silver nanoparticles are visible as dark spots inside the Cs-g-PAN/Ag nanocomposite with size approximately between 15 and 20 nm. This is appeared in the current histogram shown in Figure 2c. It is lying in the well – known nanosize range (1–100nm) which permits the composite in question to use in many medical application.

Antimicrobial activity (cup method)

Results presented in Figure 3 and Table 1 explained the antimicrobial activity of silver nanoparticles appears clearly at inhibition zone experiment against all types of microorganism. Also as listed in Figure 4 inhibition zone of (Cs-g-PAN)/Ag nanocomposite reaching 14 mm for *Pseudomonas aeruginosa* and 18 mm for *Staphylococcus aureus* and 20 mm for *Candida albicans* and 18 mm for *Aspergillus niger* and there is no inhibition for the grafted chitosan with acrylonitrile (Cs-g-PAN), these results evident the effective role of silver nanoparticles during formation of nanocomposites in the antibacterial activity of the nanocomposite towards different types of microorganisms follow the following mechanisms.

The mechanism of the inhibitory effects of Cs-g-PAN/Ag nanocmopsite on microorganisms is not completely clear, however, AgNPs interact with a wide range of molecular processes within microorganisms resulting in a range of effects from inhibition of growth, loss of infectivity to cell death which depends on shape, size and concentration of AgNPs and the sensitivity of the microbial species to silver. Several studies have reported that the positive charge on the Ag+ ion is crucial for its antimicrobial activity through the electrostatic attraction between the negatively charged cell membrane of the microorganism and the positively charged nanoparticles. In contrast, Sondi and Salopek-Sondi (2004) reported that the antimicrobial activity of AgNPs on Gram-

negative bacteria depends on the concentration of AgNPs and is closely associated with the formation of pits in the cell wall of bacteria; consequently, AgNPs accumulated in the bacterial membrane disturbing the membrane permeability, resulting in cell death. However, because those studies included both positively charged Ag+ ions and negatively charged AgNPs, this data is insufficient to explain the antimicrobial mechanism of positively charged silver nanoparticles. Amro *et al.* (2000) suggested that metal depletion may cause the formation of irregularly shaped pits in the outer membrane and change membrane permeability, which is caused by the progressive release of lipopolysaccharide molecules and membrane proteins. Although it is assumed that AgNPs are involved in some sort of binding mechanism, the mechanism of the interaction between AgNPs and components of the outer membrane is still unclear. Recently, Danilczuk and co-workers (2006) reported that Ag-generated free radicals derived from the surface of AgNPs were responsible for the antimicrobial activity. However, Lara and colleagues in another report, proposed another mechanism of bactericidal action based on the inhibition of cell wall synthesis, protein synthesis mediated by the 30s ribosomal subunit, and nucleic acid synthesis (Lara *et al.*, 2010).

Antibacterial activity against *E. coli* as pathogenic bacterium

Escherichia coli is a gram-negative bacterium of the genus *Escherichia* that is commonly found in the lower intestine of warm-blooded organisms (endotherms). Most *E. coli* strains are harmless, but some serotypes can cause serious food poisoning in their hosts, and are occasionally responsible for product recalls due to food contamination. The harmless strains are part of the normal flora of the gut, and can benefit their hosts by producing vitamin K and preventing colonization of the intestine with pathogenic bacteria.

The antibacterial activity of Cs-g-PAN/Ag nanocomposite was studied against *E. coli*, as shown in the Figure 4. The growth of *E. coli* and *S. aureus* was affected significantly by Cs-g-PAN/Ag nanocomposite compared to PAN and Cs-g-PAN copolymer. The inhibitory zone around the PAN and Cs-g-PAN copolymer is limited and cannot be observed. On the other hand, inhibitory zone could be seen clearly around the Cs-g-PAN/Ag nanocomposite. The inhibitory zone was around 16 nm in the case of *E. coli* and 15 mm in the case of S. *aureus*. The behavior can be attributed to the presence of silver nanoparticles and their antibacterial activity.

The proteomic data revealed that a short exposure of *E. coli* cells to antibacterial concentrations of AgNPs resulted in an accumulation of envelope protein precursors, indicative of the dissipation of proton motive force. Consistent with these proteomic findings, AgNPs were shown to destabilize the outer membrane, collapse the plasma membrane potential and deplete the levels of intracellular ATP.

The mode of action of AgNPs was also found to be similar to that of Ag^{+} ions; however, the effective concentrations of silver nanoparticles and Ag^{+} ions were at nanomolar and micromolarlevels (Abdel-Mohsen *et al.*, 2013).

Therefore results in *E. coli* suggested silver nanoparticles may damage the structure of bacterial cell membrane and depress the activity of some membranous enzymes, which cause *E. coli* bacteria to die eventually (Li *et al.*, 2010).

Antibacterial activity by measuring the absorbance and CFU

The results showed that the Cs-g-PAN/Ag nanocomposite were antimicrobial against *E. coli* at very low concentrations. *E. coli* strains tested (Table 2). These results were confirmed by plating the content of each well on Cs-g-PAN/Ag nanocomposite, and there was no growth for any of the strains resultant from the MIC point. The control solution without Cs-g-PAN/Ag nanocomposite did not reveal any effect on the tested bacteria.

Figure 5 shows the CFU (Counting Forming Unit) of different concentrations of (Cs-g-PAN) nanocomposite samples in comparison to control (*Escherichia coli* culture). The concentrations from 0.05 to 0.3 gm /20 ml of the growth media showing in the incubated agar plates no growth of colonies with confirmed the absorbance results (table 2). With decreasing the concentration of Cs-g-PAN nanocomposite to 0.01 gm / 20 ml of the growth media showing starting of the bacterial growth and colony forming. The inhibition reduced from 100% to 68%. These decrease in the antibacterial activity attributed to the decrease in the amount of the silver nanoparticles release from the Cs-g-PAN/Ag nanocomposite.

Acute toxicity study

Results showed no percentage mortality after 24 hours and no changes in the skin and fur, respiratory, circulatory, autonomic, central nervous systems, somatomotor activity and behavior pattern. Particular observation for tremors, convulsions, salivation, diarrhea, lethargy, sleep, and coma after 14 days of single oral administration of Cs-g-PAN/Ag at graded doses up to a 2g/ kg (Fig. 7). As 2g/ kg is not lethal, regulatory agencies no longer require the determination of an LD50 value, so the experimental doses used were 1/20, 1/40 of Cs-g-PAN/Ag (50 and 100 mg/kg).

Antibacterial effect of oral administration of Cs-g-PAN/Ag and chloramphenicol (22.5 mg/kg) on intestine *E. coli* survival in rat

As shown in Figure 6, Oral administration of 0.6mL of *E. coli* elicited intestinal infection after 3 days of its administration as compared to PBS control. As shown in Figure 8, Chloramphenicol (22.5 mg/kg) oral administration showed significant inhibition of intestine *E. coli* survival by 67.44% also, oral administration Cs-g-PAN/Ag (50 and 100 mg/kg) showed significant inhibition of intestine *E. coli* survival by 46.25 and 97.33% respectively, as compared with *E. coli* group.

Drugs were orally administered 3 days after *E. coli* administration. The surviving *E. coli* in the small intestine were quantified on the 4^{Th} day. Data were expressed as mean ± SE (n=6). Statistical analysis was carried out by one-way analysis of variance test (ANOVA) followed by the Least Significant Difference test (LSD test) for multiple comparisons; a is significantly different from PBS control at $p<0.05$; b is significantly different from *E. coli* group at $p<0.05$.

Figure 8 confirming our previous data the number of colony of the *E. coli* intestine survival for the PBS control nearly zero because there is not *E. coli* administrated while other infected rates get positive growth for the *E. coli* bacteria. *E. coli* control administered and with 600 µl of *E. coli* and untreated with any antimicrobial agent showed the highest rate of the bacterial growth nearly 360×10^6 CFU, on the other hand, the rates administrated with the same dose 600 µl of *E. coli* and treated with antimicrobial agent showed significant decrease in colony forming unit.

Table.1 Antimicrobial activity of (Cs-g-PAN/Ag) nanocomposite with concentration 0.5 gm /1 ml

Test microbe	Group	Inhibition zone (mm)
Pseudomonas aeruginosa	Bacteria G-ve	14
Staph. aureus	Bacteria G+ve	18
Candida albicans	Yeast	20
Aspergillus niger	Fungus	15

Table.2 Antibacterial activity of different concentrations of (Cs-g-PAN) nanocomposite samples in comparison to control (*Escherichia coli* culture)

Type of sample	Absorbance	Number ofCFU (10^6/ml)	Reduction %
C	2.433	4.21	0%
0.01	0.67	1.36	68%
0.05	**0.313**	**0**	**100%**
0.1	0.221	0	100%
0.2	0.225	0	100%
0.3	0.316	0	100%

Figure.1 FTIR: A) chitosan, B) chitosan –g- PAN copolymer C) Cs-g-PAN/Ag nanocomposite

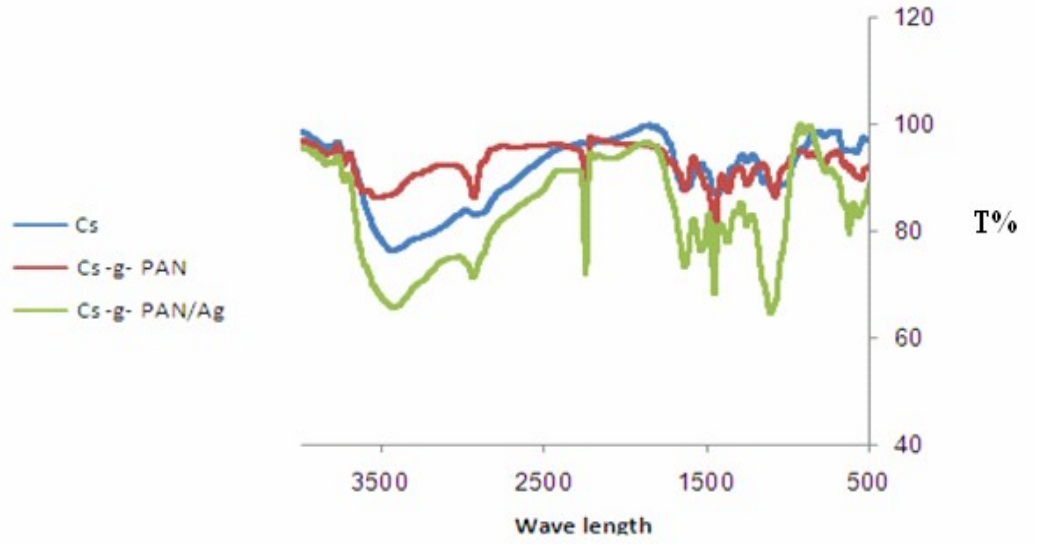

Figure.2 a) UV spectra, b) TEM images and c) Histogram of emulsion of Cs-g-PAN/Ag nanocomposite

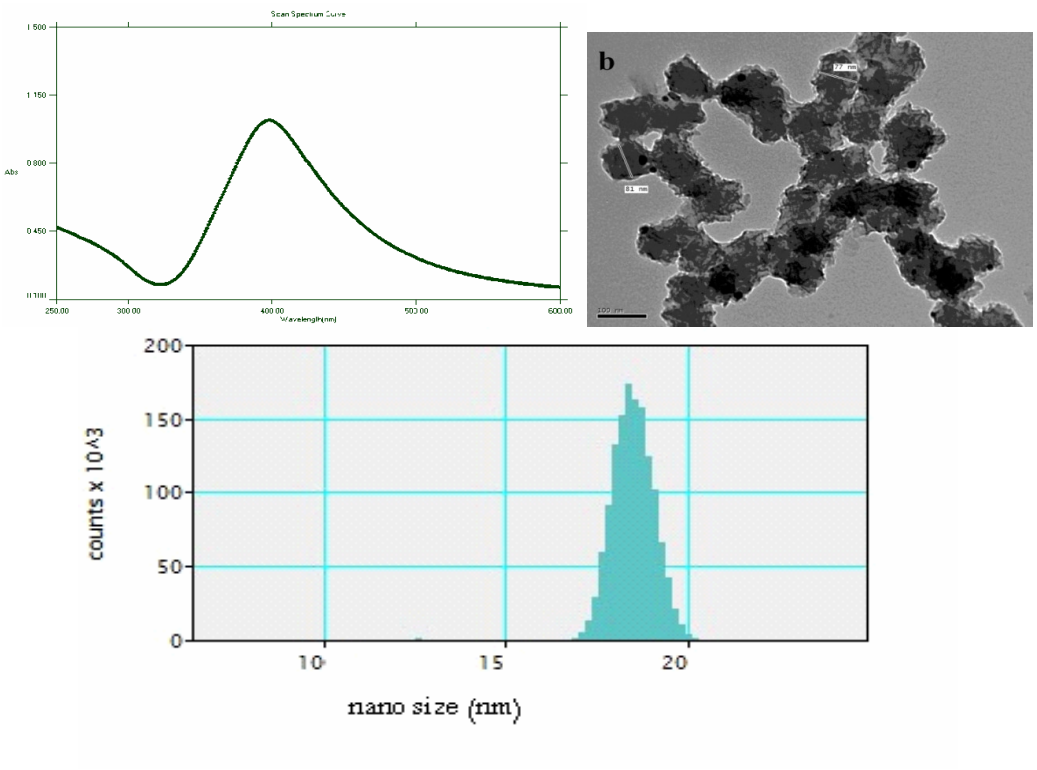

Figure.3 The antibacterial activity of Cs-g-PAN and Cs-g-PAN/Ag nanocomposite against a) *Staphylococcus aureus* (G+ve bacteria), b) (G-ve bacteria), c) *Candida albicans* (yeast) and d) *Aspergillus niger* (fungi)

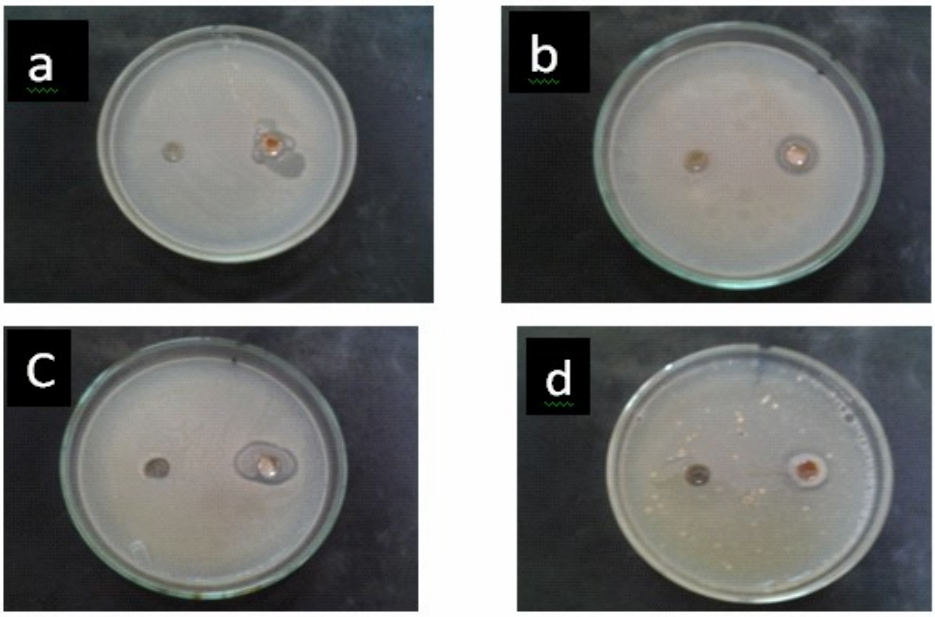

Figure.4 The antibacterial activity of PAN, Cs-g-PAN copolymer and Cs-g-PAN/Ag nanocomposite against *E. coli*

Figure.5 CFU (Counting Forming Unit) of different concentrations of (Cs-g-PAN)/Ag nanocomposite samples in comparison to control (*Escherichia coli* culture). Where; a = control, b= 0.3, c= 0.2, d = 0.1, e = 0.05, f= 0.01 (gm /20 ml)

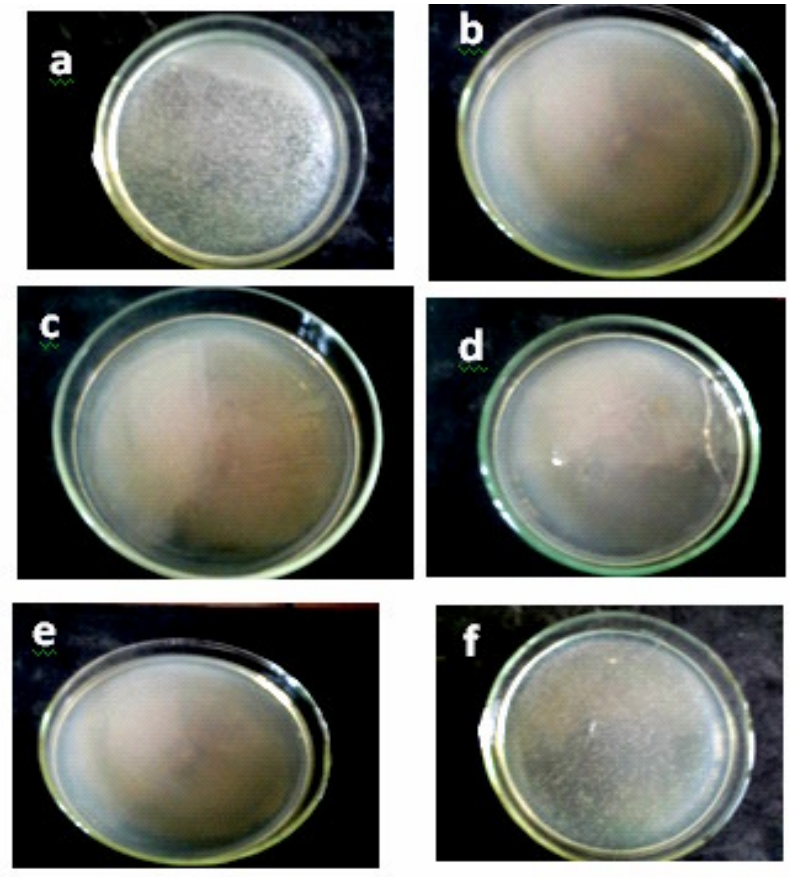

Figure.6 Illustration of the treatment schedule for antibacterial activity evaluation in vivo. b) Whole intestines of the mice infected with *E. coli* and orally dosed by gavage with PBS, Cs-g-PAN/Ag nanocomposite, and chloramphenicol (22.5 mg/kg) twice a day for three days.

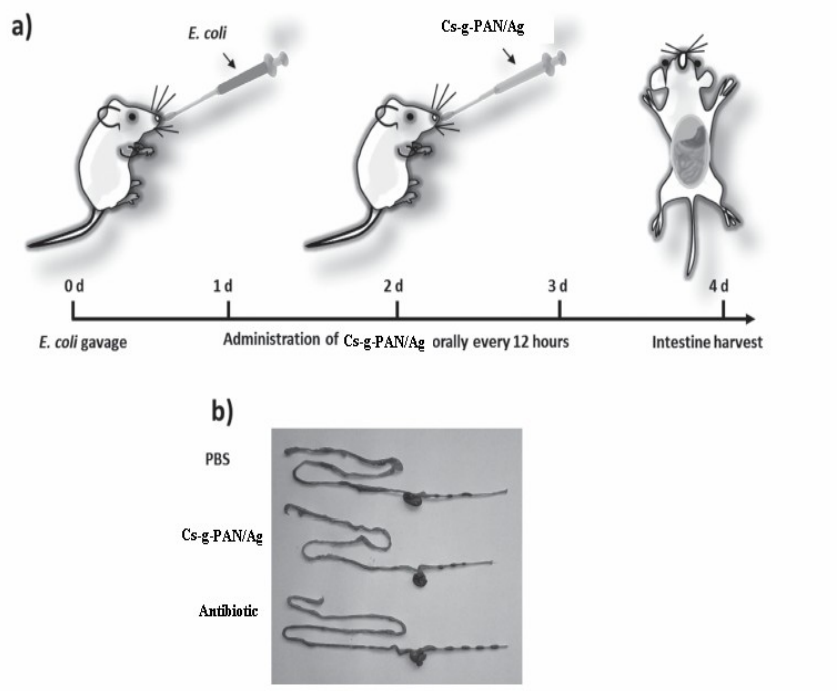

Figure.7 Antibacterial effect of oral administration of Cs-g-PAN/Ag (50 and 100mg/kg) and chloramphenicol (22.5 mg/kg) on intestine *E. coli* survival in rats

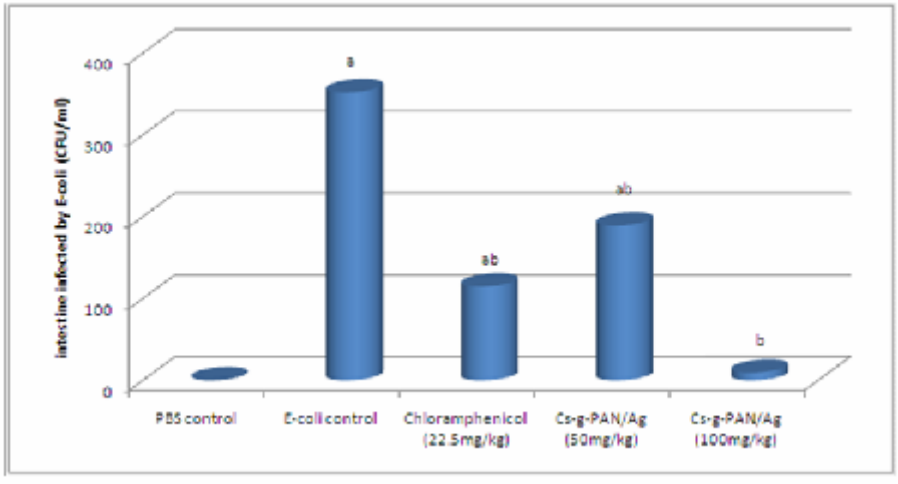

Figure.8 CFU (Counting Forming Unit) of a) infected rate; b) PBS; c) 50 mg Cs-g-PAN/Ag nanocomposite; d) 100 mg Cs-g-PAN/Ag nanocomposite; e) Chlorampheincol 22.5 mg /Kg

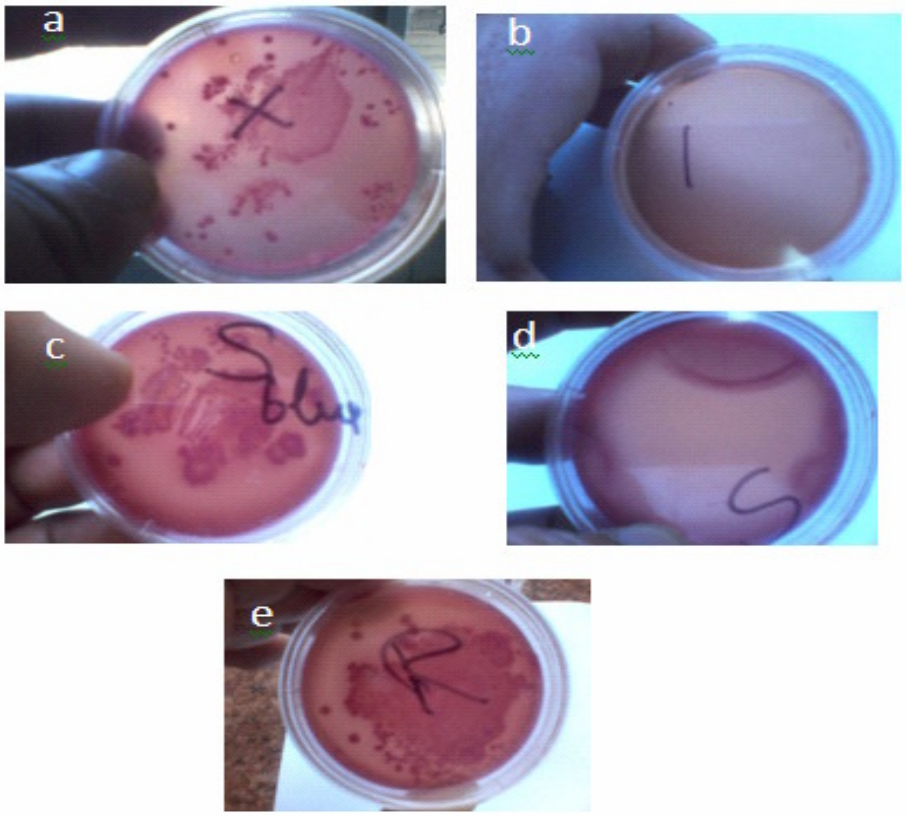

For rates treated with chlorampheincol (7.5 mg/Kg) decreased to reach 98 $\times 10^6$ CFU with inhibition 67.44%. It is noteworthy that the other samples based on Cs-g-PAN/Ag nanocomposite showed reduction in the bacterial growth connected with the concentration of administrated doses. The low dose 50 mg Cs-g-PAN/Ag nanocomposite showed 160×10^6 CFU with reduction percent reached 46.25% while the high dose 100 mg Cs-g-PAN/Ag nanocomposite showed 2×10^6 CFU with reduction percent 98%. This correlation showed the highly contact between the inhibition percent and the concentration of silver nanoparticles loaded on the nanocomposite.

The biological action of Cs-g-PAN/Ag nanocomposite against *E. coli* was investigated. MIC dose for *E. coli* inhibition and its ability to application onto animal were also studied. Other studies include antibacterial activity *in vitro* where the nanocomposite in question was submitted to cup zone test, antibacterial activity against *E. coli* as pathogenic bacteria and, determination of antibacterial activity by measuring the absorbance and CFU. Acute toxicity study was additionally undertaken. Particularly notable are that silver nanoparticles have excellent antibacterial activity against *E. coli.* This work, following previous research (Hebeish *et al.,* 2014), integrates nanotechnology and bacteriology, leading to possible advances in the formulation of new types of bactericides. However, future studies on the biocidal

influence of this nonmaterial on other Gram positive and Gram-negative bacteria are necessary in order to fully evaluate its possible use as a new bactericidal material.

References

Abdel-Mohsen, A.M., Hrdina, R., Burgert, L., Abdel-Rahman, R.M., Hašová, M., Šmejkalová, D., Kolář, M., Pekar, M., Aly, A.S. 2013. Antibacterial activity and cell viability of hyaluronan fiber with silver nanoparticles. *Carbohydr. Polymers*, 92: 1177–87.

Akinfieva, O., Nabiev, I., Sukhanova, A. 2013. New directions in quantum dot-based cytometry detection of cancer serum markers and tumor cells. *Crit. Rev. Oncol/Hematol.,* 86: 1–14.

Alivisatos, A.P. 1996. Semiconductor clusters, nanocrystals, and quantum dots. *Science*, 271(5251): 933–937.

Amro, N.A., Kotra, L.P., Mesthrige, K.W., Bulychev, A., Mobashery, S., Liu, G. 2000. High-resolution atomic force microscopy studies of the *Escherichia coli* outer membrane: structural basis for permeability. *Langmuir*, 16(6): 2789–2796.

Brigger, I., Dubernet, C., Couvreur, P. 2002. Nanoparticles in cancer therapy and diagnosis. *Adv. Drug Deliv. Rev.,* 54: 631–51.

Chan, W.C., Maxwell, D.J., Gao, X., Bailey, R.E., Han, M., Nie, S. 2002. Luminescent quantum dots for multiplexed biological detection and imaging. *Curr. Opin. Biotechnol.,* 13: 40–6.

Danilczuk, M., Lund, A., Sadlo, J., Yamada, H., Michalik, J. 2006. Conduction electron spin resonance of small silver particles. *Spectrochim Acta A Mol Biomol Spectrosc.*, 63(1): 189–91.

Forestier, F., Gerrier, P., Chaumard, C., Quero, A.M., Couvreur, P., Labarre, C. 1992. Effect of nanoparticle-bound ampicillin on the survival of listeria monocytogenes in mouse peritoneal macrophages. *J. Antimicrob. Chemother.*, 30: 173–9.

Hebeish, A., Ramadan, M.A., Montaser, A.S., Farag, A.M. 2014. Preparation, characterization and antibacterial activity of chitosan-G-poly acrylonitrile/silver nanocomposite', *Int. J. Biol Macromol.,* 68(10): 178–84.

Joguet, L., Sondi, I., Matijevi´c, E. 2002. Preparation of nanosized drug particles by the coating of inorganic cores: naproxen and ketoprofen on alumina. *J. Colloid Interface Sci.,* 251: 284–287.

Klabunde, K.J., Stark, J., Koper, O., Mohs, C., Park, D., Decker, S., Jiang, Y., Lagadic, I., Zhang, D. 1996. Nanocrystals as stoichiometric reagents with unique surface chemistry. *J. Phys. Chem.,* 100(12): 142.

Lara, H., Ayala-Núñez, N., IxtepanTurrent, L., Rodríguez Padilla, C. 2010. Bactericidal effect of silver nanoparticles against multidrug-resistant bacteria. *World J. Microbiol. Biotechnol.*, 26(4): 615–621.

Li, L.L., Wang, H. 2013. Enzyme-coated mesoporous silica nanoparticles as efficient antibacterial agents in vivo. *Adv. Health Mater.*, 2(10): 1351–60.

Li, W.R., Xie, X.B., Shi, Q.S., Zeng, H.Y., Ou-Yang, Y.S., Chen, Y.B. 2010. Antibacterial activity and mechanism of silver nanoparticles on *Escherichia coli. Appl. Microbiol. Biotechnol.*, 85(4): 1115–22.

Mattoussi, H., Mauro, J.M., Goldman, E.R., Anderson, G.P., Sundar, V.C., Mikulec, F.V., Bawendi, M.G. 2000. Self-assembly of Cdse−Zns quantum dot bioconjugates using an engineered

recombinant protein. *J. Am. Chem. Soc*., 122(12): 142.

Ramirez, J.H., Palacios, M., Tamayo, O., Jaramillo, R., Gutierrez, O. 2007. Acute and subacute toxicity of Salvia scutellarioides in mice and rats. *J Ethnopharmacol.,* 109(2): 348–53.

Richards, R., Li, W., Decker, S., Davidson, C., Koper, O., Zaikovski, V., Volodin, A., Rieker, T., Klabunde, K. 2000. Consolidation of metal oxide nanocrystals. Reactive pellets with controllable pore structure that represent a new family of porous, inorganic materials. *J. Am. Chem. Soc*., 122: 4921.

Siiman, O., Matijevi´c, E., Sondi, I. Semi conductor nanoparticles for analysis of blood cell populations and methods of making same. *U.S. Patent 6,235,540 B1*.

Sondi, I., Fedynyshyn, T.H., Sinta, R., Matijevi´c, E. 2000. Encapsulation of nanosized silica by in situ polymerization of tert-butyl acrylate monomer. *Langmuir*, 16: 9031.

Sondi, I., Salopek-Sondi, B. 2004. Silver nanoparticles as antimicrobial agent: A case study on *E. coli* as a model for Gram-negative bacteria. *J. Colloid Interface Sci.*, 275(1): 177–182.

Sondi, I., Siiman, O., Matijevi´c,, E. 2000. Preparation *of* amidodextran-CdS nanoparticle complexes *and* biologically active antibody-amidodextran-CdS nanoparticle conjugates. *Langmuir*, 16: 3107.

Srinivasan, D., Nathan, S., Suresh, T., Lakshmana perumalsamy, P. 2001. Antimicrobial activity of certain Indian medicinal plants used in folkloric medicine. *J. Ethnopharmacol.*, 74: 217–220.

Wu, X., Liu, H., Liu, J., Haley, K.N., Treadway, J.A., Larson, J.P., Ge, N., Peale, F., Bruchez, M.P. 2003. Immunofluorescent labeling of cancer marker Her2 and other cellular targets with semiconductor quantum dots. *Nat. Biotechnol.*, 21: 41–6.